Journal of Building Performance Simulation
2011, 1–18, i*First* article

Thermal zoning and interzonal airflow in the design and simulation of solar houses: a sensitivity analysis

William O'Brien[a]*, Andreas Athienitis[a] and Ted Kesik[b]

[a]*Department of Building, Civil, and Environmental Engineering, Concordia University, 1455 de Maisonneuve Blvd. West, Montréal, Québec, Canada H3G 1M8;* [b]*John H. Daniels Faculty of Architecture, Landscape, and Design, University of Toronto, 230 College St., Toronto, Ontario, Canada M5T 1R2*

(*Received 8 June 2010; final version received 25 September 2010*)

Many assumptions must be made about thermal zoning and interzonal airflow for modelling the performance of buildings. This is particularly important for solar homes, which are subjected to high levels of periodic solar heat gains in certain zones. The way in which these passive solar heat gains are distributed to other zones of a building has a significant effect on predicted energy performance, thermal comfort and optimal design selection. This article presents a comprehensive sensitivity analysis that quantifies the effect of thermal zoning and interzonal airflow on building performance, optimal south-facing glazing area, and thermal comfort. The effect of controlled shades to control unwanted solar gains is also explored. Results show that passive solar buildings, in particular, can benefit from increased air circulation with a forced air system because it allows solar gains to be redistributed and thus reduces direct gain zone overheating and total energy consumption.

Keywords: building energy simulation; passive solar houses; thermal zoning; airflow; thermal comfort

1. Introduction

The predictably periodic nature of solar radiation – both diurnally and seasonally – makes it particularly suitable for reducing the purchased energy of buildings. This is especially true for low-rise residential buildings (e.g. detached houses), whose loads are envelope – dominated and whose occupants are able to adapt to small temperature swings, since clothing choice, location within the building and activity level are somewhat flexible.

Solar buildings are defined as those that offset a major portion of their energy use with solar energy collection – both passive and active. In short, solar buildings attempt to maximize utilizable solar gains during the heating season, while minimizing them in the cooling season. The relatively short, but intense periods of wintertime solar gains are passively moderated with high levels of thermal mass. Thermal comfort issues – particularly overheating or the cooling to mitigate it – pose a major design constraint and are often the limiting factor of glazing area.

During the early design stage of solar buildings, the main issues of interest include relative performance (e.g. energy use, resource use and costs) and the diagnosis of any major problems such as overheating and other sources of thermal discomfort. These potential risks should be identified early, when there is the greatest opportunity to make cost-effective design changes (Reed and Gordon 2000). While the early design stage usually implies simplistic models with many unresolved design details, the issues of thermal zoning, controls and airflow should be carefully considered. Solar building performance models require particular attention because of the unbalanced nature of the heat gains, which at times can overheat one zone despite the fact that others are being mechanically heated.

While the two issues of thermal zoning and interzonal airflow may appear to be distinct, they are merely at opposite ends of a continuous spectrum: magnitude of interzonal energy exchange. For instance, infinite airflow between two zones (complete, instantaneous mixing) is equivalent to merging them into one zone. The effect of heat transfer from interzonal airflow (convection) relative to interzonal conduction can be quantified, as follows, for convection and interzonal conduction, respectively.

$$U_{12,\mathrm{air}} = \dot{m}\, C_{\mathrm{p}} \tag{1}$$

$$U_{12,\mathrm{wall}} = \frac{A}{2/h_c + R} \tag{2}$$

*Corresponding author. Email: w_obrie@encs.concordia.ca

ISSN 1940-1493 print/ISSN 1940-1507 online

DOI: 10.1080/19401493.2010.528031
http://www.informaworld.com

Equation (1) defines the rate of energy that can be moved between zones by means of airflow on a per unit of temperature difference between them basis. Equation (2) defines the rate of energy that is transferred between two adjacent zones' air (defined by their air nodes) and is inversely proportional to the thermal resistance of the wall, including the convective heat transfer coefficient. The two different modes represented by the equations are illustrated in Figure 1. If two zones are separated by a partition wall with closed openings (e.g. doors), the only means for heat transfer are by conduction through that wall or mechanically driven systems, such as ducts. It should be noted that the impact of interzonal airflow on heating and cooling loads is the same whether it is caused by natural or forced convection.

A sample calculation for common wall configurations demonstrates that the energy transferred by airflow is typically much more significant than conduction between zones. For instance, an airflow rate of 400 L/s yields allows the transport of 480 W/K assuming the air has specific heat capacity of 1 kJ/kgK and a mass density of 1.2 kg/m^3. This airflow rate is typical for residential forced-air systems (Chen *et al.* in press a,b). A partition wall made of wood studs (400 mm on centre) sandwiched between two layers of 13-mm gypsum with a convective heat transfer coefficient of 2.0 W/m^{2}K and that is 2.74 m tall and 10 m wide (the size of the interzonal walls in the case study that follows) has a steady state conductance (between adjacent air nodes) of about 19 W/K. Thus, for these two examples, the convective mode is about 25 times as effective as conduction at transferring energy between zones. Merging two zones into one (represented by a single air node) is infinitely more effective because the air temperature is assumed constant throughout a zone (Clarke 2001).

There are two main approaches to modelling interzonal airflow: CFD (computational fluid dynamics) (microscopic) and airflow networks (macroscopic) (ASHRAE 2005). CFD provides (and requires) significant detail about geometry and boundary conditions. In contrast, airflow networks provide an efficient and comprehensive means to analyze airflow in buildings (Hensen 1991) and perform energy and thermal comfort studies at early stage design. Airflow networks are driven by buoyancy, wind and mechanical forces. They consist of nodes (state of each node is pressure), which are connected by airflow components (openings, cracks and ducts). Conservation of mass and energy is applied. Airflow networks reduce the amount of required information about airflow paths/obstacles and surfaces. During early stage design, when the effect of major design parameters such as aspect ratio, glazing area, and insulation levels are being established, room layout may not be known. There is no certainty regarding opening geometry (e.g. interior door positions) and assuming that they are all optimally positioned could be optimistic (in terms of air mixing). Therefore, despite having a wide range of methods for assessing the impact of airflow within a building, a modeller may not have sufficient knowledge about the building to properly apply them. The literature suggests that most building performance models with detailed airflow networks are applied to buildings that are either built or whose interior geometry is established (Warren 1996, Sahlin 2003, Simonson 2005). For the built buildings, measured airflow characteristics such as air leakage are often used as inputs to the airflow model – clearly something that cannot be performed during early stage design.

Natural convection can be promoted between zones of a building in several ways, ranging from doorways and fixed openings to convective loops

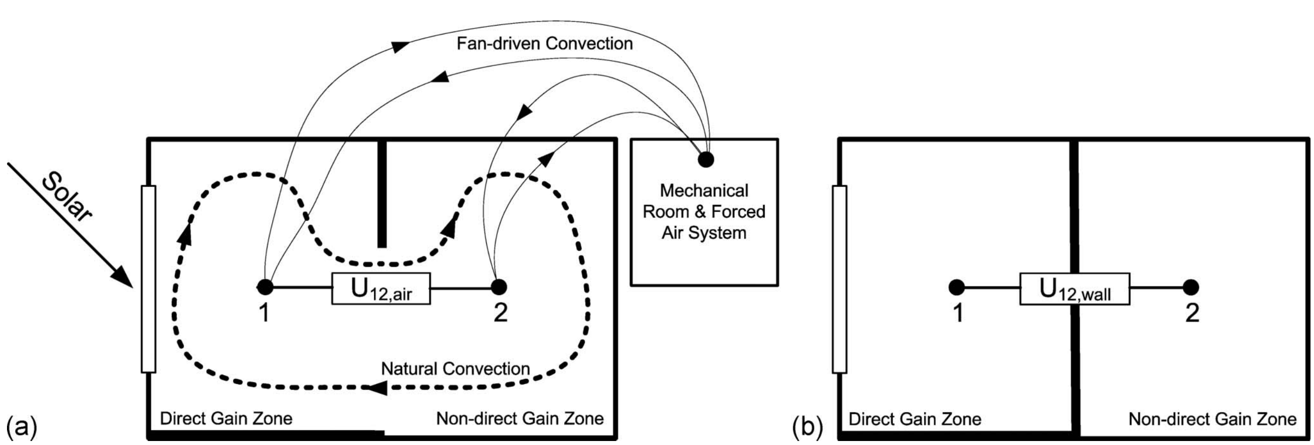

Figure 1. Different modes for heat transfer: via convection – mixed forced and natural convection (left) and conduction through a partition wall (right).

(Balcomb 1983). The latter technique is particularly effective because it provides a continuous path, made of hallways and stairwells, for air to circulate between all zones. This occurs naturally as the air in the direct gain zone is heated and rises to the top of the zone where it may leak into other rooms. This air is replaced at the bottom of the direct gain zone by cooler air, which again, could come from other zones. Balcomb *et al.* (1977) reports total measured airflow rates through doors of between 0.3 and 1.05 m^3/s during sunny periods, corresponding to energy transport up to 6 kW. This is equivalent to the peak incident solar radiation (about 1000 W/m^2) on 12 m^2 of glazing (for south-facing glazing with a solar heat gain coefficient of 0.5).

Recent technological developments of low-cost multi-zone forced air systems with heat pumps can be configured to circulate air between zones, even when no heating or cooling is required. This can facilitate the circulation of hot air from the direct gain zone to colder parts of the house (see e.g. Athienitis 2007). For example, the Canadian Advanced House in Brampton circulates air at 285 L/s for this purpose (Hestnes *et al.* 2003). Similarly, the EcoTerra house circulates air at about 400 L/s (Chen *et al.* in press a,b). For both cases, the fan in the central forced-air system is used at a constant rate, depending on the mode under which it is operating (e.g. heating, cooling, or circulation). Electronically commutated motor (ECM) fans can be operated over a wide range of airflow rates and have been shown to achieve flow/power ratios as high as nine times greater than permanent split capacitor motor fans in circulation mode (Gusdorf *et al.* 2010). Through long-term measurements of a house, Gusdorf *et al.* (2010) found that an ECM fan consumed just 16.5 W in circulation mode, at an airflow rate of 211 L/s. For modelling and design purposes, mechanically driven airflow can be imposed with a greater level of certainty and control than that from natural convection alone. Unlike for natural convection, the airflow path, connections to the building, and airflow rate are known for mechanically driven air circulation (Feustel and Dieris 1992, Warren 1996).

For modelling, a building should be subdivided into thermal zones such that a zone is attributed to each region with significantly different boundary conditions, loads, controls, and/or operating conditions. If higher resolution is required (e.g. knowledge of temperatures in a particular region of a building), further subdivision of zones is also appropriate. While early approaches for modelling houses used single-zone models, multizone models with interzonal airflow were developed to study individual heating and cooling loads and for the study of the distribution of air contaminants (Warren 1996). Guides for energy modelling tools, such as that for EnergyPlus (US DOE 2009), suggest that the number of thermal zones represent the number of HVAC distribution units serving the building. Often, HVAC control zoning provides cues about thermal zoning (ASHRAE 2005). In houses, using forced-air or hydronic distribution systems, it is possible to independently control zones with different needs (e.g. bedrooms, kitchen and living room) using thermostatically controlled dampers or valves (NRCan 2010). For example, the Belgian PLEIADE row house described by Hestnes *et al.* (2003) has four independently controlled zones. The literature indicates that there are instances of houses with between two and eight control zones being used in solar houses (see e.g. Galloway 2004, Athienitis 2007). The EnergyPlus manual (US DOE 2009) states that building modellers should avoid assigning a zone to each room of a building, though it admits that the task of zoning is an art form. Greater discretization of a space requires increased model input time, simulation time, and, more importantly, additional specification of interzonal heat transfer.

Many building energy simulation programs for houses [e.g. HOT3000 (CANMET CETC 2008) and BEopt (NREL 2009)] model the entire above-grade occupied space as a single zone, thus assuming that the air throughout the house is well mixed. This may be suitable for typically glazed, solar neutral homes [those with equal glazing area on all facades (Hayter *et al.* 2001)], but is less so when significant heat gains only occur in certain zones. Thus, the appropriate attribution of thermal zones to model buildings with passive solar features is an important area of research.

While the use of more control zones offers the advantage that thermal comfort can be maintained to a higher degree of resolution, it occurs at the expense of additional equipment and distribution costs. However, this can be at least partially offset with smaller ducts equipment and operating costs. For example, the Athienitis house (Athienitis 2007) is programmed to operate only one of the stages of the two-stage heat pump during periods when only one zone requires heating or cooling.

This article quantifies the importance of paying careful attention to thermal zoning and interzonal airflow, especially early in the design. A solar house of fixed geometry (except for window and overhang size) is simulated under many different configurations to demonstrate the impact of modelling assumptions on predicted performance and optimal design. The results of the study show that both thermal zoning and interzonal airflow not only have an impact on predicted heating and cooling energy, but also on the optimal building design. Controlled shades significantly reduce loads at high levels of glazing and are a key contributor to the mitigation of overheating. General conclusions are drawn from the case study to be applied to other solar building designs and their modelling approaches.

2. Methodology

The purpose of this work is to quantify the effect of the rate of mechanically driven air circulation and thermal zone assignments. The use of dynamic whole-year simulations allows a comprehensive sensitivity analysis to be performed such that relationships can be directly established.

The tool that was used, EnergyPlus, has the capability of using an implicit finite difference method, which is particularly suitable for buildings with high levels of thermal mass. The fundamental formulation of the finite difference method that it uses is as follows:

$$\rho c_{\mathrm{p}} \Delta x (T_{i,\mathrm{new}} - T_{i,\mathrm{old}})/\delta t = k(T_{i-1,\mathrm{new}} - T_{i,\mathrm{new}})/\Delta x + k(T_{i+1,\mathrm{new}} - T_{i,\mathrm{new}})/\Delta x \tag{3}$$

The left-hand side represents the change in stored energy in the node over the time interval δt. The right-hand side represents the energy that is conducted towards the current node. Its magnitude is dependent on the conductivity of the material k, the thickness of the control volume Δx, and the difference between the current node temperature and the neighbouring node. Each nodal temperature is labelled by node position relative to the current node i and for either the current timestep (new) or the previous timestep (old). The layer thickness is automatically selected to satisfy Fourier stability criteria. Equation (3) is created for each node, including surface nodes, material interface nodes, and nodes that are internal to each material layer. EnergyPlus uses the Gauss–Siedel iteration scheme to solve the system of implicit equations (EnergyPlus 2009).

To determine each zone's air temperature, an energy balance is performed on each zone's air node at each time step and the amount of heat required to be added or removed to maintain the zone air temperature between the specified range is calculated (EnergyPlus 2009). Since an ideal system (with infinite capacity) was used, this amount of heat is added or subtracted from each zone air node. Once this amount of heat is calculated, the current zone air temperature is calculated using Equation (4), in which the zone air energy balance is solved for the current temperature T_Z^t and the transient term (resulting from the thermal capacity of the air and non-surface zone contents) is approximated by a third-order Taylor series expansion of the Euler formula. The justification for this approach, and particularly the fact that the third-order approximation is used, is thoroughly explored by Taylor *et al.* (1990).

$$T_Z^t = \frac{\sum_{i=1}^{N_{\mathrm{sl}}} \dot{Q}_i + \sum_{i=1}^{N_{\mathrm{surface}}} h_i A_i T_{\mathrm{s}i} + \sum_{i=1}^{N_{\mathrm{zones}}} \dot{m}_i c_{\mathrm{p}} T_{\mathrm{z}i} + \dot{m}_{\mathrm{inf}} c_{\mathrm{p}} T_\infty + \dot{m}_{\mathrm{sys}} c_{\mathrm{p}} T_{\mathrm{supply}} - A}{\left(\frac{11}{6}\right) \frac{C_z}{\delta t} \sum_{i=1}^{N_{\mathrm{surfaces}}} h_i A_i + \sum_{i=1}^{N_{\mathrm{zones}}} \dot{m}_i c_{\mathrm{p}} + \dot{m}_{\mathrm{inf}} c_{\mathrm{p}} + \dot{m}_{\mathrm{sys}} c_{\mathrm{p}}} \tag{4}$$

$$A = \left(\frac{C_{\mathrm{z}}}{\delta t}\right)\left(-3T_{\mathrm{z}}^{\mathrm{t}-\delta \mathrm{t}} + \frac{3}{2} T_{\mathrm{z}}^{\mathrm{t}-2\delta \mathrm{t}} - \frac{1}{3} T_{\mathrm{z}}^{\mathrm{t}-3\delta \mathrm{t}}\right) \tag{5}$$

In Equation (4), all terms that contribute to the zone air energy balance are on the right side, including heat sources, heat exchange with the surfaces that enclose the zone, air exchange with other zones, air exchange with the outside (i.e. infiltration), and input from the HVAC. Furthermore, the right side contains the effect of the zone air energy storage from the previous three timesteps [Equation (5)].Transmitted solar radiation is distributed on interior surfaces based on EnergyPlus 'full interior and exterior with reflections' algorithm for insolation and shading, which calculates an hourly distribution for each month of the year (EnergyPlus' 2009). Unlike the simpler algorithms, which assume all transmitted direct solar radiation is incident on the floor, this one traces it to determine which surface it hits. Any reflected shortwave radiation is redistributed among the other interior surfaces based on view factors. Similarly, diffuse solar radiation from the sky or reflected from the ground or other exterior surfaces is apportioned by the view factors. If a window shade is present, it is assumed a perfect diffuser, resulting in hemispherically uniform diffuse radiation. This level of detail is important for a building model in which the role of thermal storage and the solar radiation that is incident on it is so fundamental to successful performance.

For this case study, a 300 m^2 (100 m^2 per storey including the basement), two-storey (plus basement)

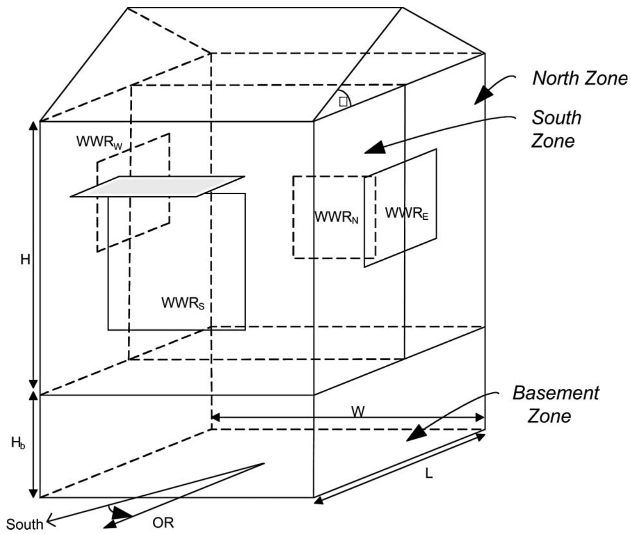

Figure 2. Energy model for the three-zone configuration.

Table 1. Modelled parameter values.

Parameter	Value
$W = L$	10 m
H	5.5 m
H_b	2.5 m (1.0 m of which is above grade)
WWR_S	Variable; 0.05–0.8
$WWR_E = WWR_N = WWR_W$	0.05
Glazing type	Double-glazed, low-e, argon-filled; U-value = 1.802; SHGC = 0.586
Frame U-value	1.82 W/m^2K (insulated vinyl)
Glazing edge to centre-of-glass conductance ratio	1.63
OR	0 deg (South-facing)
Basement slab resistance	3 m^2K/W
Basement wall resistance	3 m^2K/W
Wall resistance	8 m^2K/W
Ceiling resistance	10 m^2K/W

house in Toronto was modelled in EnergyPlus version 5.0 (US DOE 2009). This size was selected to represent a typical North American suburban detached house. Toronto experiences cold sunny winters and warm humid summers, making the seasonal adaptability of the house critical and challenging. A diagram of the house is shown with the variable parameters (Figure 2). The parameters were fixed for all simulations, except for south-facing window area, zonal configuration, interzonal airflow rate, overhang depth, and the presence of controlled shades. The key parameter values are summarized in Table 1. Note that several references to south in the paper correspond to the northern hemisphere; however, all results can be applied to the southern hemisphere (in which case the glazing would be predominantly north facing).

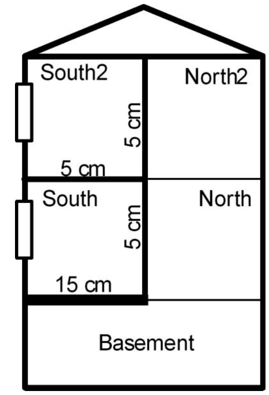

Figure 3. Thermal mass location and thickness.

The house is high in thermal mass with the thickness of the medium-density concrete illustrated in Figure 3. All other walls (interior and exterior) are a typical wood-frame construction. The concrete slabs were modelled in layers with a thickness of 2.5 cm, and this is later assessed for sensitivity. The number of simulation timesteps per hour was set at 30, as recommended, to minimize simulation time (EnergyPlus 2009). South-facing window-to-wall ratios (WWR_S) of between 0.05 and 0.8 were examined to assess nearly all possible design options. This range corresponds to a solar aperture (window area to total floor area ratio) of between 0.91 and 14.7%. Simulations were run for increments of WWR_S of 0.075. Windows were modelled to be congruent (i.e. same height-to-width ratio) to their parent surfaces. Windows were modelled with a frame area to glazing area ratio of 0.25 and whose thermal and optical properties were determined using WINDOW5 software (Huizenga *et al.* 2005). A combined air infiltration and ventilation rate was fixed at 0.15 air changes per hour (ach). Low-energy airtight houses can achieve an air leakage rate of 0.5 ach (at 50 Pa) (see e.g. Chen *et al.* in press a,b, Hestnes *et al.* 2003) or about 0.025 ach at normal conditions (Sherman 1987). A ventilation rate of 0.3 ach and a heat recovery ventilator (HRV) effectiveness of 60% results in an equivalent of 0.12 ach.

The overhang geometry was selected to prevent shading in the winter while shading the majority of the glazing in the summer. Specifically, they were sized to be both: (1) deep enough to completely shade the bottom of the glazing at solar noon on summer solstice [Equations (5)] and (2) shade none of the glazing at solar noon on the winter solstice [Equation (6)]. These constraints yield a unique solution for overhang depth and overhang height above the top of the glazing. This is illustrated in Figures 4 and 5. It should be noted that any glazing that is permanently shaded necessarily has a net heat loss during the heating season; thus, it is extremely important to design any fixed shading devices to ensure this does not occur. The overhang width was matched to the glazing width.

$$\tan(\alpha_{\min}) = h_{\mathrm{OH}}/d_{\mathrm{OH}} \tag{6}$$

$$\tan(\alpha_{\max}) = (h_{\mathrm{OH}} + h_{\mathrm{g}})/d_{\mathrm{OH}} \tag{7}$$

As houses become more tightly sealed and better insulated, internal heat gains from people and non-HVAC power-consuming equipment play an increasingly significant role in the energy balance. For the case study, the house was assumed to be occupied by four people on weekdays from 18:00 to 6:00 and for all hours on weekends. Non-HVAC–related energy consumption (and consequently, heat gains) was assumed to total 4800 kWh per year. This is in line with conservative occupant behaviour as defined by Armstrong (2009). The gains were distributed over a daily schedule in accordance with Armstrong's synthetically derived profile, which features peaks in the morning and evening. Specially, the gains were distributed amongst the zones by floor area.

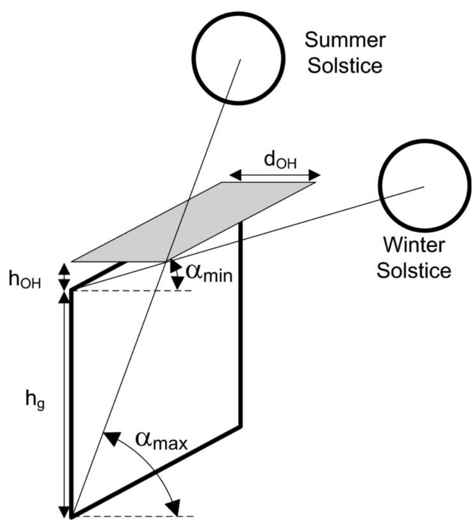

Figure 4. Overhang geometry with key parameters.

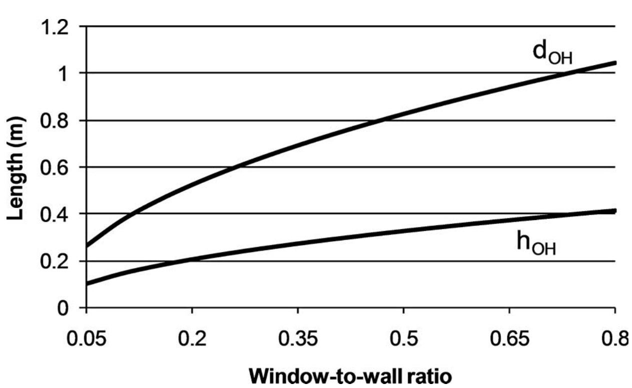

Figure 5. Overhang depth and height above glazing as a function of window-to-wall ratio.

2.1. Controls

Controls are critical for solar houses and must attempt to maximize solar energy utilization while maintaining thermal comfort. By definition [see Equation (8)], no sensible thermal storage can occur without a change in temperature; thus, the temperature in a building must be allowed to swing if solar gains are to be used to offset future purchased energy. Since the thermal mass and air node temperature are not necessarily equal (but usually similar), it is possible for the mass to store a modest amount of energy without a zone air temperature change. For instance, in the morning, the solar radiation on the thermal mass initially heats it before the energy is convected to the air. The greater the thermal mass, the more potential there is for it to undergo a temperature change without having adverse effects on the zone air temperature; namely overheating.

$$\Delta C = \Delta T \rho V_c \tag{8}$$

The HVAC configuration used for this study is shown in Figure 6(a). It uses a common set of ducts to supply conditioning and ventilation to each zone. Such a configuration saves on both equipment costs and on volume for ductwork. The airflow to each zone is controlled by a damper such that heat can be added or removed as required to maintain the desired temperature. Heat is added or removed from the air in the air-handling unit (AHU), as needed. The exhaust air from each zone is partly exhausted to the outdoors, before which some of its heat is recovered by the HRV, and partly returned to the AHU. However, to simplify the model for the case study, ideal controls were used, such that heat and coolness were injected into the occupied zone(s) at the air node whenever needed. The modelling tool used allows infinite heat or coolness injection into the air node, when ideal controls and systems are used. The 'Ideal Loads Air System' in EnergyPlus was used. It is a variable air volume (VAV) system that allows a variable airflow rate to satisfy the cooling or heating load. It should be noted that this airflow does not affect the interzonal airflow rates or mass balance considered in the model. The modelled configuration is shown in Figure 6(b). While this approach is simpler to implement and provides considerable flexibility, its limitations should be noted. First, it neglects pressure drops, heat transfer, and leakage from ducts. Second,

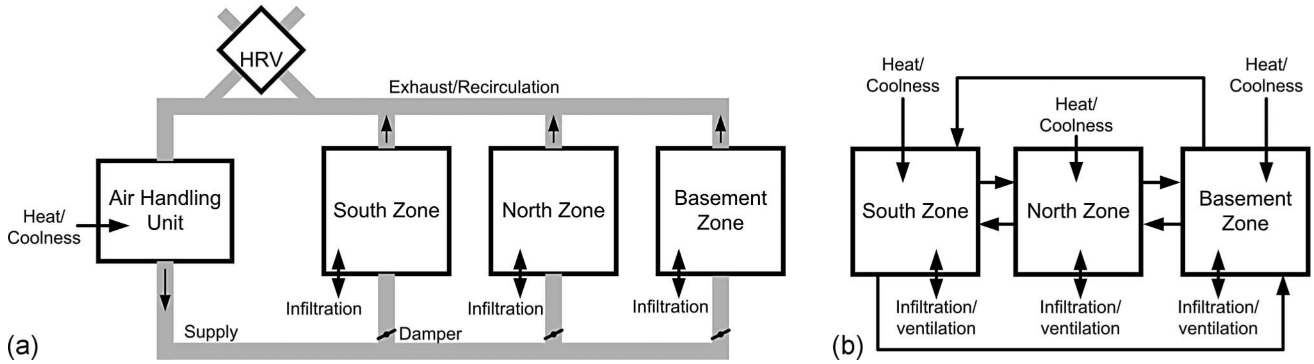

Figure 6. (a) The intended HVAC system, including AHU, zoning, and distribution. (b) The modelled HVAC system, showing all major heat transfer and airflow phenomena.

the modelled configuration assumes a constant rate of air mixing, whereas in reality, there are some occasions when not all of the zones require heating or cooling and their dampers would be closed. This modelling assumption is considered valid because the frequency at which this occurs is low and when it does occur, the benefit to increased airflow (described later) is insignificant because heating tends to be needed in all zones during periods of low solar gains (when interzonal airflow is less beneficial) (Figure 6).

To prevent unrealistically high rates of heat injection or removal such that they remained below the capacity of typical residential systems, any increase in control temperature setpoint was ramped up linearly between an hour before the change to an hour after the change. This eliminated any large heating spikes.

The controls maintain the zonal air node temperature between 20 and 26°C, except at night (10 pm to 7 am) when the heating setpoint was set back to 18°C. This time is typically when occupants are sleeping and prefer cooler temperatures. The literature suggests that nighttime setbacks of between 15 and 20°C be used for passive solar houses (Besant *et al.* 1979, Hestnes *et al.* 2003, Chen *et al.* in press a,b, NRCan 2010). The nighttime setback has two purposes: (1) delay the time at which heating must be supplied at night, which ultimately reduces heating energy and (2) provide a greater capacity to store solar gains before overheating occurs, as indicated by Equation (8). Mechanical cooling was only allowed between May 1 and September 30, during the expected cooling season. Thus, brief shoulder period overheating was possible. In fact, solar houses are most prone to overheating in the shoulder seasons; particularly autumn when temperatures remain mild and the solar altitude is low and allows signficant solar gains (Athienitis and Santamouris 2002).

During the heating season, solar gains should be admitted and temperatures should be allowed to rise to the maximum level at which the occupants are comfortable in order to maximize the amount of stored thermal energy. However, if no heating is expected to be required for the next day, a means of minimizing solar gains should be implemented, to prevent the possibility overheating.

Free cooling was modelled by introducing outdoor air into each zone at a rate of 1.2 m^3/s. Rates of 0.5–1.7 m^3 are typical for fans for the purpose of free cooling (Galloway 2004). Free cooling was enabled if the following conditions were met.

- $T_z > 25.5°C$
- $T_{amb} < 20°C$
- $30\% > RH_{amb} > 60\%$

The first restriction is to prevent outdoor air from being introduced if overheating is not occurring (with a margin of 0.5°C below the cooling setpoint). The second restriction prevents air that is nearly as warm as the indoor air from being introduced, since the fan power consumption is unlikely to be justified for any temperatures above this value. Similarly, the third restriction avoids the introduction of latent heat to the house.

As mentioned, because of the seasonal lag between peak daily solar altitude and mean daily temperature, autumn overheating can occur in highly glazed houses. Overhangs are not effective at preventing this because the solar altitude is relatively low (Hestnes *et al.* 2003). An effective solution to this problem is a movable shading device. Window blinds or shades have been shown to also improve thermal comfort by preventing direct solar radiation. For instance, Newsham (1994) found that the presence of controlled blinds reduced the predicted percent of people dissatisfied with the thermal environment from 22 to 13%. For the study, interior shades on south-facing windows were controlled during the period from April 1 through October 31, such that they closed if incident solar radiation on the exterior of the window exceeded 150 W/m^2 and an outdoor temperature of 20°C; otherwise, they were left open. These values were found to be suitable for consistently minimizing cooling while avoiding the rejection of useful solar gains in the shoulder seasons. Thresholds for closing shades in the literature have been suggested to be between 150 and 250 W/m^2 (Newsham 1994, Hestnes *et al.* 2003). Movement of shade positions can either be realized through automated control with motorized shades or through a diligent occupant. The shades were modelled with a reflectance of 0.8 and a transmittance of 0.1, in accordance with EnergyPlus' standard high reflectance, low transmittance shade (US DOE 2009). The algorithms for determining the optical and thermal effects (including the convective heat transfer between the shade, cavity air and zone air) of the shades are described in detail in the EnergyPlus Engineering Reference document (EnergyPlus 2009).

It is important to note that the results that follow are premised on a heating/cooling system with individual zone controls. In new Canadian houses, a single thermostat is often employed for forced air heating/cooling systems. If there is only a single zone, thermostat location is a critical factor in establishing the actual operation of the heating/cooling system. If the thermostat is located in a direct-gain zone where passive solar gains are high, the other zone(s) will remain at much cooler temperatures because heating will not be triggered. Energy savings will be achieved at the cost of thermal comfort. Assumptions regarding the controls for the heating/cooling system and interzonal air circulation are critical to accurate modelling of actual thermal performance.

2.2. *Zonal configurations*

As mentioned, the act of assigning thermal zones is often considered an art form and thus is explored here in detail to quantify its sensivity. For the case study, four different zonal configurations were examined for the house energy model, while the interzonal airflow was set to zero. The models are otherwise geometrically and thermally identical. All floors and partition walls were modelled for all configurations to maintain equivalent thermal mass and isolation patterns. This was done by using the same five-zone model and applying an adequately high rate of airflow (10 m^3/s) between appropriate zones, such that the zone temperatures remained within 0.05°C of each other. This effectively merges the zones into a single zone, while allowing the interior thermal mass and interior solar distribution to be explicitly modelled. All other interzonal airflow was set at zero for this part of the study. Windows were distributed equally among zones on each façade (i.e. equal area on first and second floors). The roof (assumed an unoccupied attic) was modelled as a thermal zone but not counted in the naming convention, as it was only thermally linked to the other zones via conduction; not airflow. The diagrams are shown in Figure 7.

The different configurations were selected to examine possible control zones and to reflect different common modelling tendencies. The three and five zone configurations provide information about finely controlled, advanced houses, such as those referenced in the literature review. The three and five zone configurations can also be used to conservatively model overheating, since they effectively isolate the direct and non-direct gain zones from each other.

2.3. *Interzonal airflow*

For the case study, specific airflow rates were explicitly imposed by a forced air system fan. Such systems are efficient, low-cost, and enable a higher level of certainty than natural convection, as discussed in the literature review. Three interzonal airflow rates were examined, including 0, 200 and 400 L/s (0, 424 and 848 CFM), representing typical values of low-energy houses discussed in the literature review. For all of them, air from

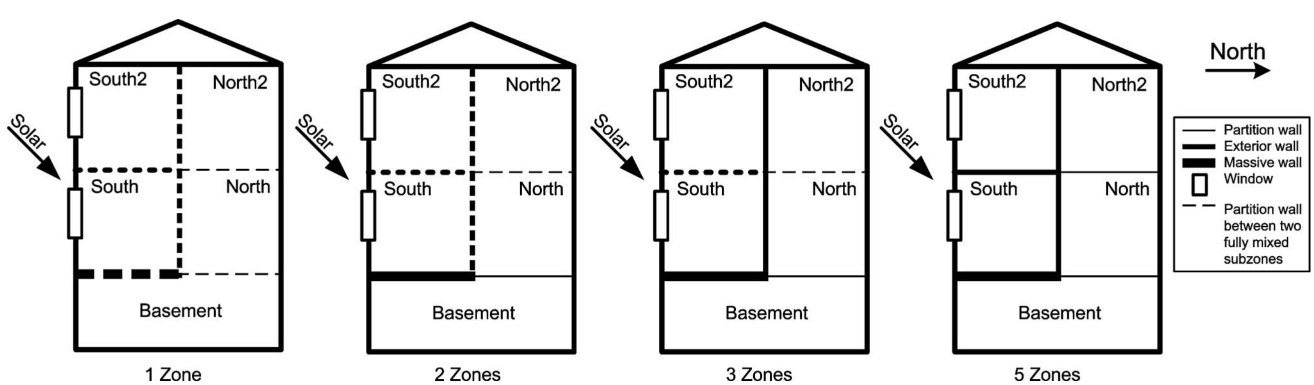

Figure 7. Zonal configurations for one, two, three, and five zones.

each occupied zone was returned to the AHU, where it is assumed to be mixed, and re-supplied equally to each zone. To properly represent the effective airflow rate, the real configuration [Figure 6(a)] must be compared to the modelled configuration [Figure 6(b)]. A volume flow balance was used to calculate how much of the air leaving each zone enters the other two. Starting at the AHU, if 200 L/s is blown by the fan, one-third or 67 L/s enters each zone assuming the system is balanced and is in re-circulation mode. Because of the conservation of mass, approximately the same amount of air leaves each zone, assuming that infiltration balances exfiltration. The exhaust air from each zone merges and is partly exhausted; 0.3 ach of ventilation is equivalent to 67 L/s for the 800-m^3 house. Therefore, two-thirds of the air re-entering the AHU is exhaust air from the zones and the remaining third is fresh air. Assuming this air is perfectly mixed, the air entering each zone is one-third fresh air, and two-ninths is from each of the three zones. It is therefore concluded that the four-ninths of the mechanically driven airflow actually causes effective interzonal airflow, while the remainder either distributes fresh air or merely returns exhaust air to the zone in which it originated. Thus, for the current model and the 200 L/s case, each pair of zones exchanges 44 L/s (two-ninths of 200 L/s). This same ratio is applicable to all interzonal airflow rates.

For the three airflow rates examined, the 0 L/s case could represent a house with radiant floor or baseboard heating in which air is not the primary heat distribution medium, while the non-zero cases represent forced air systems. While the air is constantly circulated for these simulations, a control system that limits fan use to periods of significant interzonal temperature differences is advisable to save fan energy. The results are shown for the three-zone configuration only, but general conclusions can be extended to all multi-zone configurations.

This work is most applicable to houses with forced-air distribution systems, in which heat or coolness are delivered via ducts and returned to the system through returns, as previously described. The fan(s) could conceivably be used more effectively if the air were circulated directly between the direct gain and non-direct gain zones without mixing it first, thus eliminating the airflow that is merely returned to the zone from which it originated. Furthermore, the warm air should be taken from the top of the direct gain zone. Such advanced configurations are the subject of future research.

2.3. *Performance metrics*

Two metrics are used to quantify the house's performance: annual space conditioning energy (which includes that required to maintain the aforementioned comfort conditions, resulting from all transmission or heat gain phenomena related to the envelope, ventilation, infiltration, solar gains, equipment and people) and overheating. The cost per unit of heating and cooling was assumed to be equal. This is most suitable for two common equipment configurations: (1) a heat pump with similar coefficients of performance (COPs) for heating and cooling, or (2) an electric air conditioner with a COP of about 3 for cooling and a fossil fuel-based (e.g. natural gas) furnace for heating. In the latter case, the primary energy input per unit of heat added or removed to the space is approximately equal. For instance, North America's primary energy input to secondary energy output ratio is approximately 3 (Deru and Torcellini 2007), but varies by region and time. But, if the per unit cost of cooling were less than heating, for instance, this would tend to increase optimal glazing areas.

Preliminary results were found to be particularly sensitive to the definition of overheating. Typically, overheating is quantified by the number of hours above 25 or 28°C (see e.g. CMHC 1998, Robinson and Haldi 2008). However, this definition is not suitable for this research because it does not allow proper comparison between the different zonal configurations. In the multi-zone configurations, simultaneous differences of 5°C or more are not uncommon. Furthermore, merely measuring the number of hours above a certain temperature neglects the fact that higher temperatures are less comfortable than those just above this threshold. Interestingly, it was found that merely measuring the hours above 26°C would indicate that circulating air is adverse, in some instances, because it leads to more zones being over the threshold – though barely. However, overall comfort conditions under these conditions would, in fact, be improved by most standards. Thus, a new metric was devised to account for all of these considerations. It is hour-degrees (Celsius) above 26°C multiplied by the floor area fraction of the house. For example, if 80% of the floor area of the house is at a temperature of 28°C for 1 h and the rest is below or equal to 26°C, this would contribute 1.6 hour-degrees [i.e. 1 h, 80%, (28–26°C)].

Since mechanical cooling is modelled as ideal and is permitted in the five warmest months, overheating can only occur at other times of the year. The event of daytime overheating and nighttime mechanical heating during the heating season is an indication of a missed opportunity to effectively store passive solar gains, excessive window area, and/or ineffective circulation of air in the house.

The key weather data, zone air temperatures, and heating loads are shown for a sample sequence of days (14–16 March) for the three-zone configuration in Figure 8. The sequence contains one cloudy day followed by two clear days with spring-like temperatures. The south-facing window to wall ratio was set at 50% – a level that may cause overheating to exceed satisfactory conditions but that was selected for demonstration. No mechanical or passive cooling measures were taken so that the possibility of overheating can be demonstrated. Airflow rates of both 0 and 200 L/s are shown for comparative purposes. The graphs indicate that if the zones are isolated (in terms of airflow) instantaneous temperature differences of 10°C are possible under sunny conditions. Furthermore, if the zones are individually controlled, heat is still required for the basement zone, despite the fact that the direct gain (south) zone overheats. In contrast, if airflow between the zones is mechanically imposed at 200 L/s, the zone temperatures remain within 3°C of each other. Furthermore, heating is not required after the morning of the second day of the sequence. The two heating load peaks for each day represent: (1) the heat injection required to increase the zone air temperature from the nighttime setpoint to the daytime setpoint and (2) the heating required to maintain the daytime setpoint several hours after sunset, as the passively stored heat cannot keep up with envelope losses. The heating energy for the period is 27.6 and 26.1 kWh for the 0 and 200 L/s cases, respectively. It is worth noting that the peak heating load on the first day of the sequence is briefly higher in the case with greater interzonal airflow. This is an artifact of the previous day, on which a moderate amount of solar gains occur, such that the direct gain zone stores some energy, but not enough to eliminate heating loads in the other zones. In the high airflow case, the energy from the solar gains is redistributed, despite the fact that it is all required in the direct gain zone. Thus, the direct gain zone, which has the highest envelope heat losses because of its large glazing area, requires a significant amount of heat to raise its temperature to the daytime heating setpoint. This indicates that interzonal airflow is particularly beneficial for clear days and particularly for the purpose of reducing the magnitude of overheating. Clearly, given that the outdoor temperatures are low during the period, the direct gain zone temperature would be lowered by introducing more fresh air. However, this is wasteful considering the other zones still require heating. The analysis presented here is useful for understanding the physical phenomena that occur when interzonal airflow is introduced.

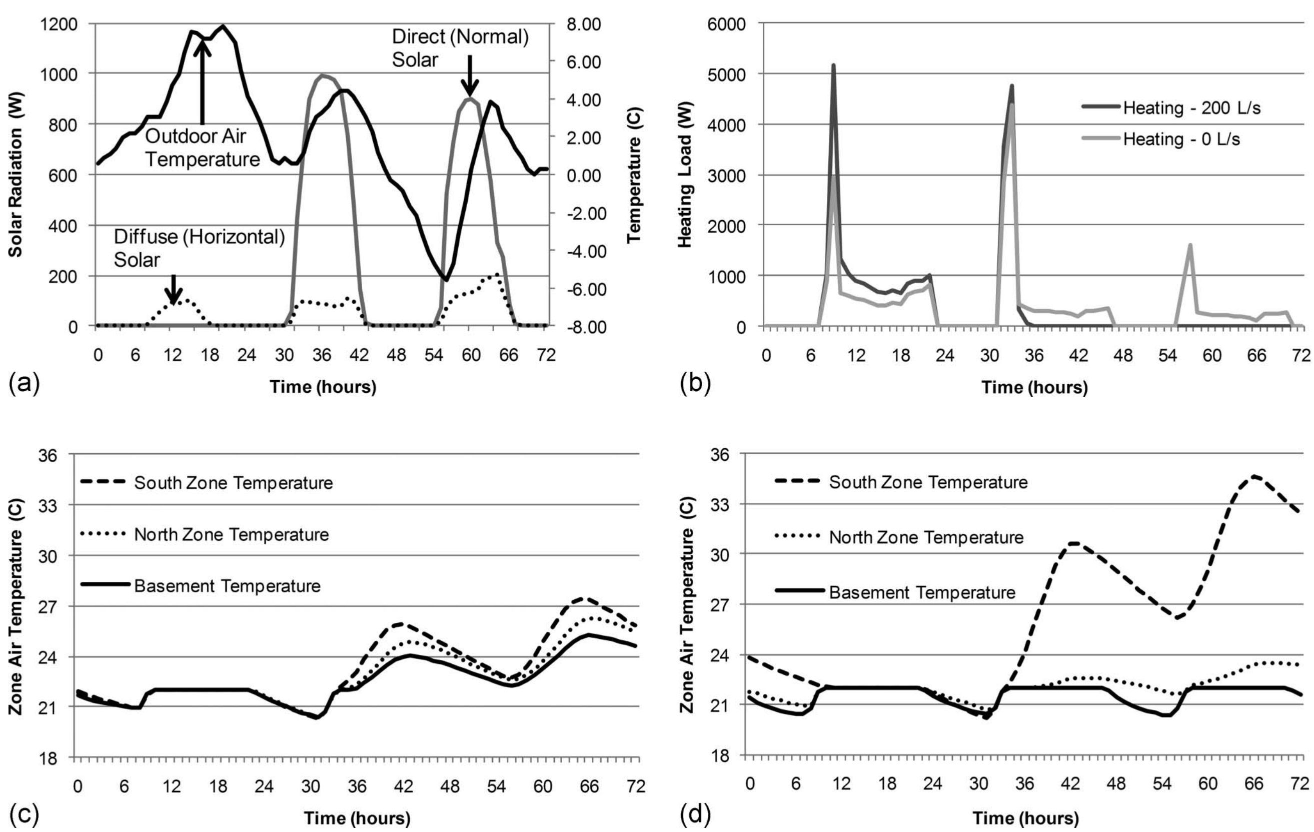

Figure 8. The performance of the house model for the cases 0 and 200 L/s of interzonal airflow during a three-day sequence: (a) weather conditions, (b) heating loads, (c) zone air temperature profiles for the 200 L/s case, and (d) zone air temperature profiles for the 0 L/s case.

Figure 9 provides a specific case of temperature distributions in the house for the three-zone configuration. It shows that circulating air reduces heating needs and improves comfort by distributing the solar gains throughout the house. While the heating energy actually increases in the direct gain zone when airflow is increased, this is more than made up for in the basement zone. The results show that with increased air circulation, the heating and cooling energy is reduced by a total of 16% while the magnitude of overheating is reduced by 55%. Note that here, and only here, overheating is quantified by hour-degrees above 26°C (without the zone volume accounted for), since the behaviour of individual zones is displayed. The remainder of this study focuses on annual results, since this period represents an entire climatic cycle.

3. Results

Results are shown in the form of a sensitivity analysis. They indicate both the effect of zonal configuration and interzonal airflow and of different values of WWR_S. This shows the effect in terms of magnitude as well as optimal WWR_S. WWR_S was selected as the key parameter because it is fundamental to passive solar performance and exhibits an interesting U-shaped curve, which is unseen for the majority of other parameters, such as insulation levels and infiltration rates. The primary results are followed by the results of a sensitivity analysis on a critical selection of some of the model assumptions and design choices.

3.1. Number of zones

Figure 10 shows the heating and cooling energy for the four different zonal configurations, with both no shades present and controlled shades. The results show that the models with more zones are consistently predicted to underperform relative to those with fewer zones. This is because heating is frequently used in the non-direct gain zones, even if the direct gain zone(s) is/are overheating. The configuration with just one or two zones implies that the solar-heated air is well mixed throughout the house, thus using their heat capacity and making up for the heat losses in non-direct gain zones. The curves for the three and five-zone models are similar because both of them isolate the direct gain zone(s) from the rest of the house. Thus, the extra effort to discretize the south side of the house may not be justified. Similarly, the results suggest that the use of a single above-grade zone would be sufficient for houses with small glazing areas.

Interestingly, the presence of controlled shades causes the curves to flatten out for higher values of WWR_S. This indicates that shades are able to reject much of the unwanted solar gains and minimize the cooling energy. However, the benefit of shades is primarily seen for values of WWR_S that are above the optimal level, and are thus mainly necessary if large windows are desired. While the minimum combined heating and cooling energy with and without controlled shades is similar, the presence of shades allows for larger windows without facing overheating.

South

Airflow rate (L/s)	Over-heat (h•°C)	Peak Temp. (°C)	Heating energy (kWh)	Cooling energy (kWh)
0	5898	37.8	804	1201
200	1168	31.3	974	1071
400	1015	30.8	983	1052

North

Airflow rate (L/s)	Over-heat (h•°C)	Peak Temp. (°C)	Heating energy (kWh)	Cooling energy (kWh)
0	381	29.3	1257	458
200	888	30.3	926	419
400	1013	30.3	923	417

Basement

Airflow rate (L/s)	Over-heat (h•°C)	Peak Temp. (°C)	Heating energy (kWh)	Cooling energy (kWh)
0	1	26.2	879	2
200	716	29.5	491	16
400	787	29.8	488	18

Figure 9. Example results for a house with a WWR_S of 0.5, three zones, and different air circulation rates. Each table refers to the thermal behaviour of its specific zone. All other conditions are as previously described for the nominal design.

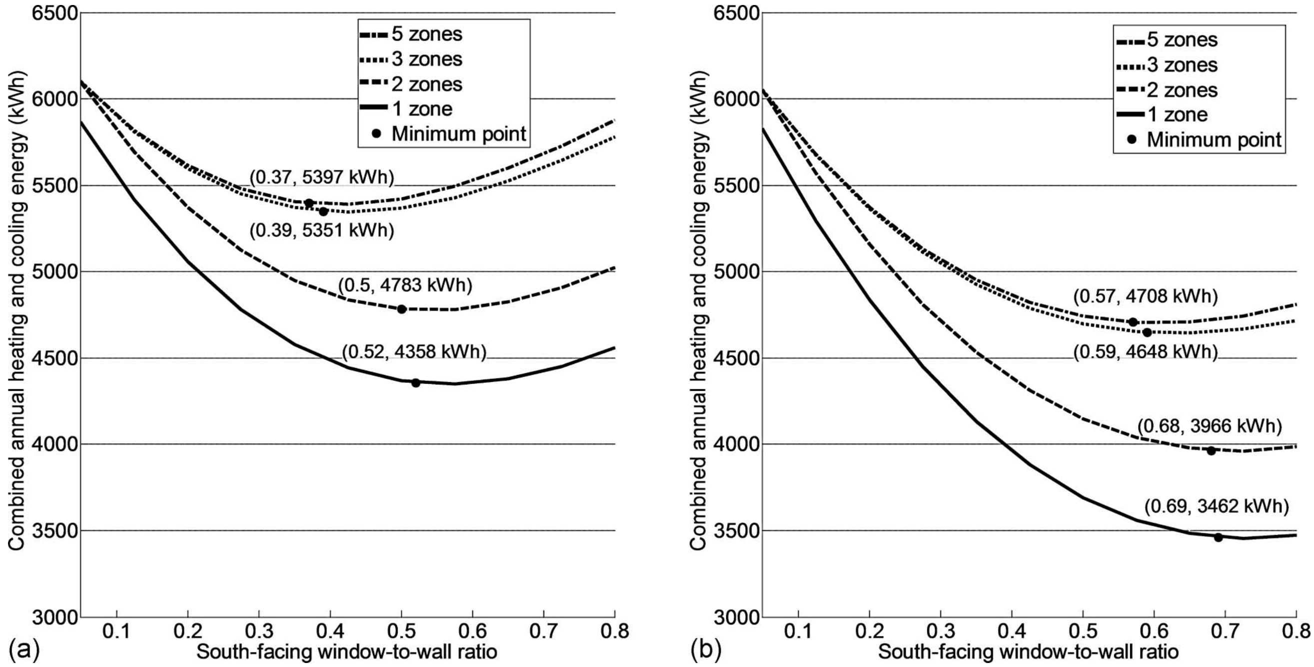

Figure 10. Effect of number of zones on energy without shades (left) and with shades (right).

Therefore, the other benefits of large windows – namely, views to the outdoors and daylighting – are possible without the cost of additional energy consumption.

For the case with no shades, the zonal configuration affects the optimal WWR_S by 15% points, thus illustrating the effect on optimal design. The effect is more pronounced for the case with shades as it indicates that, at least for the one and two zone configurations, a WWR_S that is as large as practically possible is optimal. That is, the benefit of additional passive solar heating outweighs the additional cooling energy. However, these conclusions can only be made for controlled shades and the effect would be lessened for shades that were less strictly controlled.

Figure 11 indicates that household overheating is most significant for the configurations with more zones. This is because having a greater number of zones isolates the solar gains, which prevents the use of the non-direct gain zones' thermal mass. It also leads to more overall heat injection because the non-direct gain zones may require heating even if the direct gain zone(s) overheat. The presence of controlled shades significantly reduces the magnitude of overheating, though it is still clearly an issue for larger glazing areas.

3.2. *Interzonal airflow*

Under the three-zone configuration, in which different interzonal airflow rates were explored, a similar though subtler trend to the number of zones exists, relative to the zoning configuration. Using airflow to distribute solar gains decreases loads and increases optimal glazing area. The results indicated that increasing airflow provides diminishing returns for energy savings, since most of the benefit is achieved from 0 to 200 L/s, and that there is little benefit to increasing this to 400 L/s (see Figure 12). Again, the presence of shades flattens the curve for higher glazing areas, indicating minimal change from adding glazing beyond the optimal level. Note that the curve for 0 L/s is identical to that for three zones in Figure 10, since the study on zonal configurations uses zero interzonal airflow.

Figure 13 reiterates the fact that increasing airflow provides diminishing returns. The temperature profiles indicate that increasing air circulation is most effective during times when the direct gain zone overheats and the other zones require heating. During periods of high solar gains and mild temperatures, if all of the zones begin to overheat, circulation offers little benefit, other than equalizing the temperatures, which may or may not be desirable. Again, the ability of shades to prevent overheating is evident when the two graphs are compared.

3.3. *Sensitivity analysis of assumptions*

To demonstrate the sensitivity of several of the other model assumptions and design options, simulations were performed under the three-zone configuration with 200 L/s of interzonal airflow. The effect of a selection of factors on the heating and cooling energy

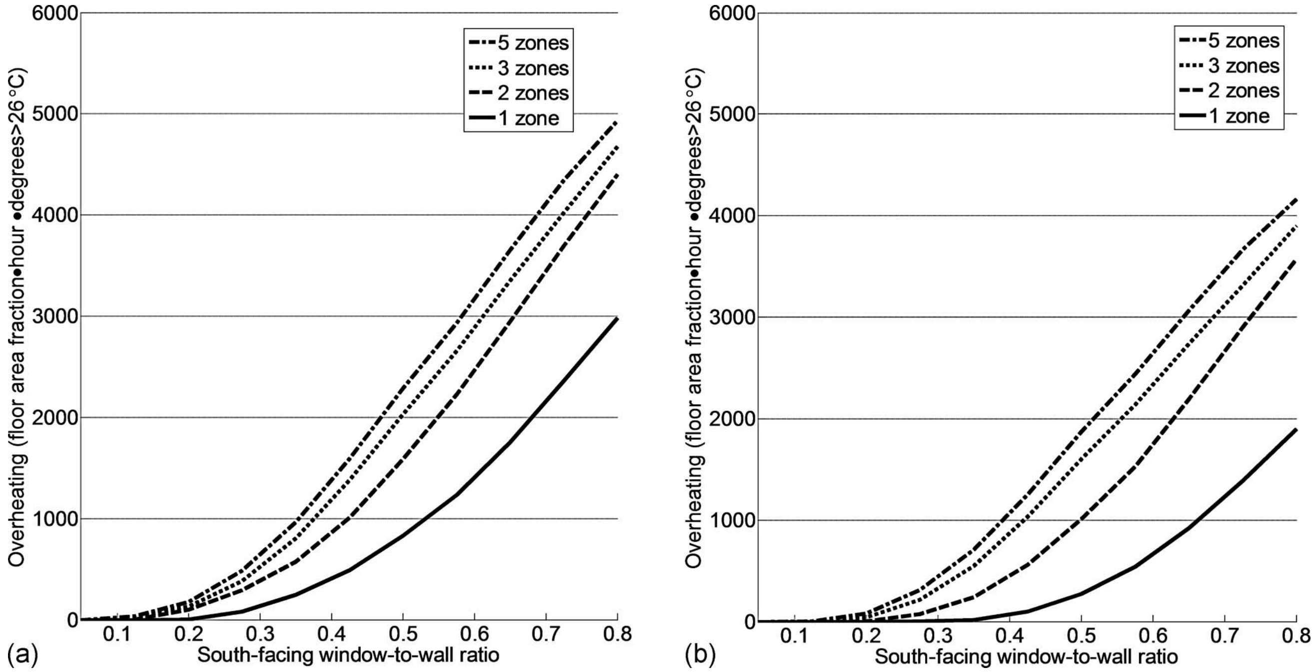

Figure 11. Effect of zones on whole house overheating without shades (left) and with shades (right).

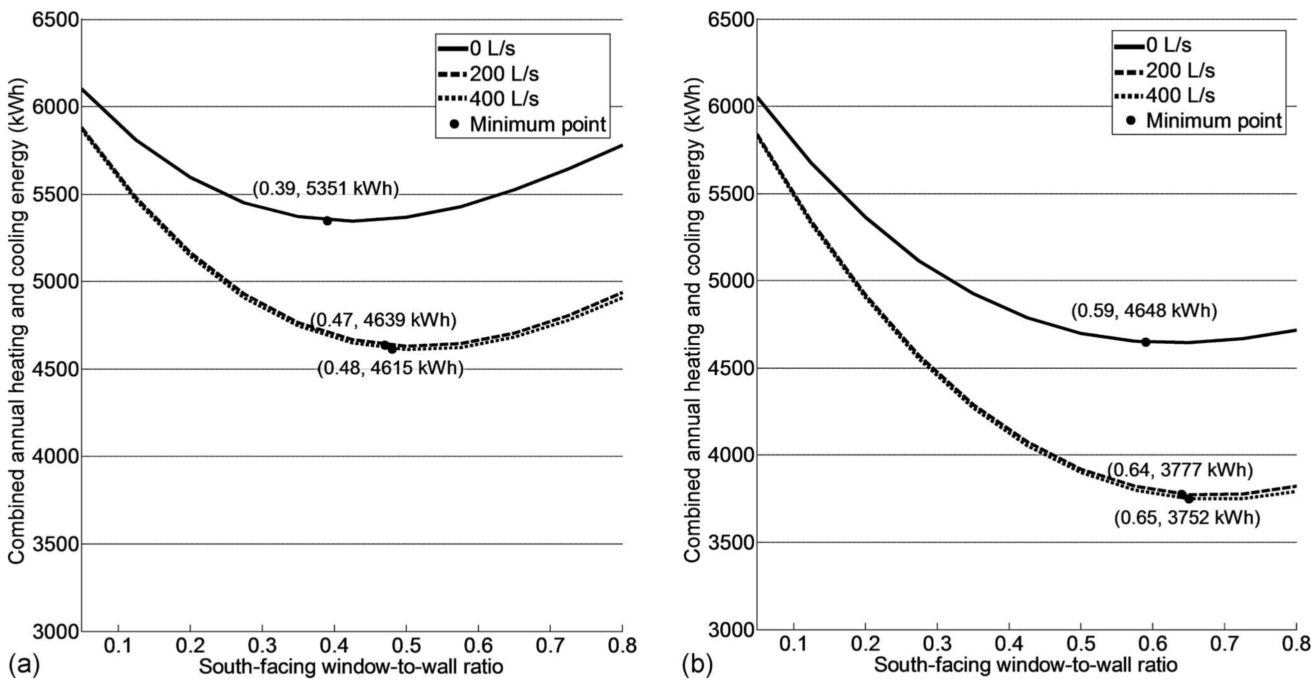

Figure 12. Effect of airflow rate on energy without shades (left) and with shades (right). Note that the curves for 200 and 400 L/s are nearly coincident.

and the magnitude of overheating was explored, with each variation explained as follows. Simulations were run for the entire range of south-facing glazing areas, as previously defined.

Nominal: as described in the Methodology section; with three zones and 200 L/s of interzonal airflow. Specifically, the nighttime setpoint is 18°C, the cooling setpoint is 26°C, the overhang depth is as previously described, the concrete slab in the south zone is modelled with layers with thicknesses of 2.5 cm, the simulations are run at 30 timesteps per hour, and the double-glazed low-e, argon-filled windows.

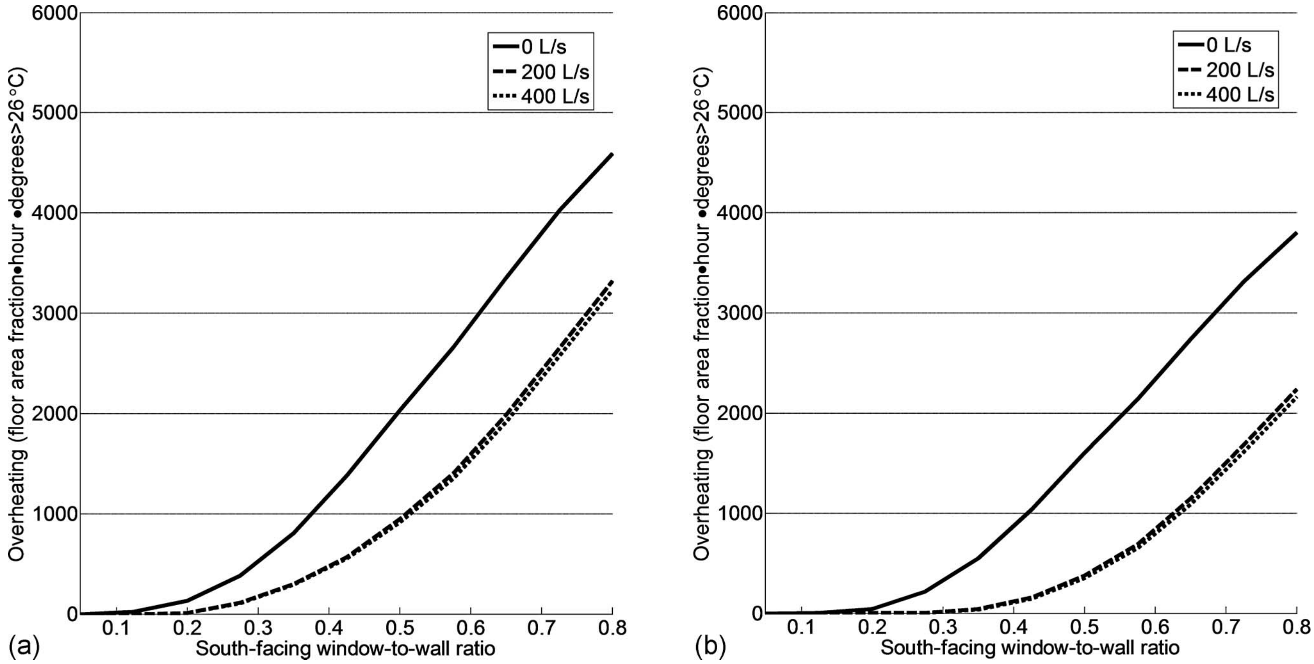

Figure 13. Effect of airflow rate on whole house overheating without shades (left) and with shades (right). Note that the curves for 200 and 400 L/s are nearly coincident.

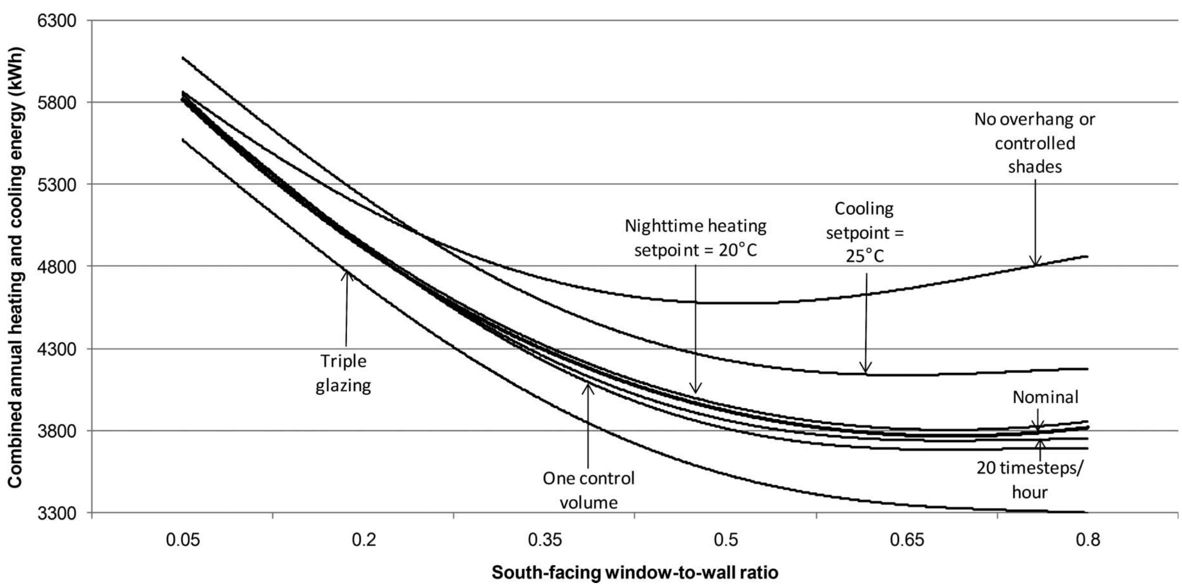

Figure 14. Effect of a selection of assumptions on heating and cooling energy.

Nighttime setpoint = 20°C: There is no nighttime setback, thus the heating setpoint is a constant 20°C.

Cooling setpoint = 25°C: The cooling setpoint is lowered to 25°C during the cooling season.

No overhang or controlled shades: No overhang is present and the shades are left permanently open.

One control volume for thermal mass: The concrete slab on the floor of the south zone is modelled as a single control volume.

Twenty timesteps/hour: Simulations are run at 20 timesteps per hour – the lowest level recommended by the EnergyPlus Engineering Reference Manual (EnergyPlus 2009).

Triple-glazed windows: The double glazing is replaced with triple glazing with two low-e coatings and argon-filled cavities. This change applies to all windows – not just the south-facing window.

The results of the simulations are Figure 14. The results indicate that the effects of time and space

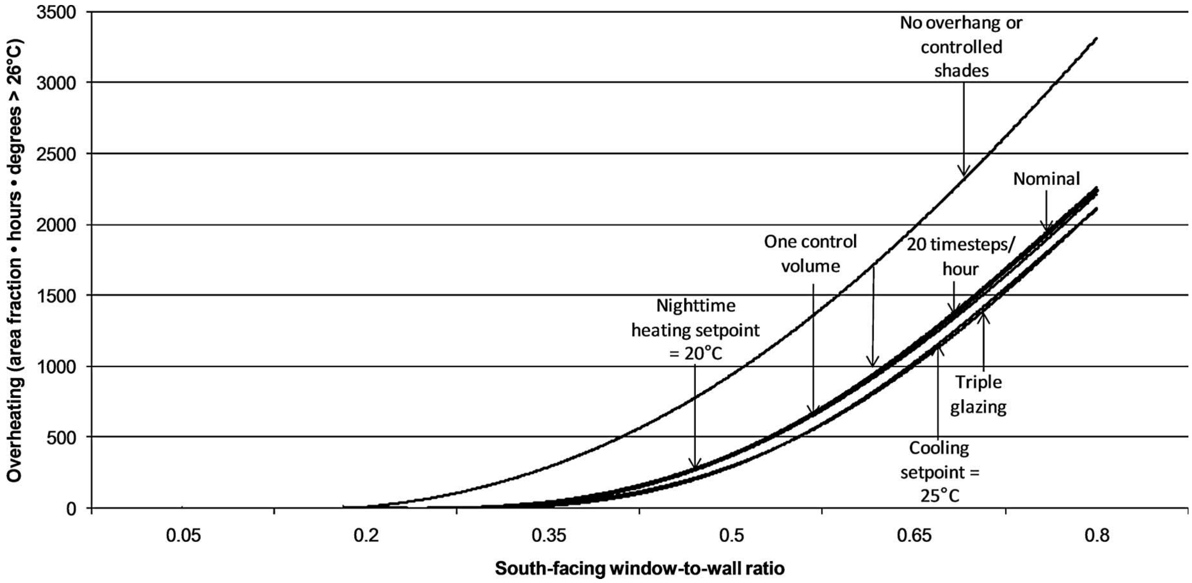

Figure 15. Effect of a selection of assumptions on overheating.

discretization are minimal. Narrowing the deadband of the temperature setpoints results in a significant increase in conditioning energy, as expected. Interestingly, increasing the nighttime heating setpoint has minimal impact. Further analysis showed that the zone temperature rarely reached the nighttime setpoint; owing to the air-tightness, high levels of insulation and thermal mass, and the internal gains. In contrast, reducing the cooling setpoint significantly increases the energy consumption of the house. This further demonstrates that increasingly strict thermal comfort expectations tend to result in poorer thermal performance. The presence of an overhang and shading control is particularly important for large south-facing windows. The change of glazing reduces the energy use for all glazing areas explored and the effect is most pronounced for larger south-facing window to wall ratios. The difference, even for the smallest south-facing window size, is a result of the fact that the non-south windows were also changed for this aspect of the sensitivity analysis.

The effect of the same items on overheating is shown in Figure 15. The results suggest that the discretization of space and time and the nighttime setpoint have little effect on overheating. However, the presence of an overhang is effective at reducing overheating – particularly for large glazing areas. The negligible impact from changing the cooling setpoint is because overheating does not occur during the cooling season (when the cooling setpoint is used), as explained by the section that describes the controls.

4. Conclusions

The results show that assumptions about both thermal zoning and airflow can significantly affect predictions of energy performance, thermal comfort, and the optimal design. Restricting interzonal airflow or modelling a building with a large number of zones reduces the optimal south-facing glazing area because solar gains are not properly distributed within a building and are not as effective at reducing purchased heating and direct gain zone overheating. In the cases without shades, the assumptions about thermal zoning and airflow affected the combined heating and cooling energy by 14 and 19%, respectively. Similarly, these same effects changed the optimal south-facing window-to-wall ratio by 20 and 9 percentage points, respectively. While early energy models cannot be expected to perfectly match measured results, a non-optimal glazing area (or other design parameter) represents a missed opportunity to reduce energy use.

It should be noted that the absolute results of this work cannot be directly applied to other situations unless all assumptions, thermal properties, and the climate are the same. The severity of overheating is dependent on glazing area, overall envelope thermal resistance, internal heat gains, and shading – active or fixed. Thus, the appropriate airflow rate depends on the significance of the imbalance of heat gains and losses for each zone. However, results are expected to be applicable in relative terms. From the results of this work, it is recommended that building performance modellers perform the following analyses for buildings with unbalanced heat gains (e.g. passive solar houses or buildings with isolated equipment heat gains).

(1) The sensitivity of thermal zone discretization over a practical range should be assessed, noting that having more zones is a more conservative, though more time-consuming, approach. The thermal zoning schemes necessary for other aspects of building performance simulation, such as daylighting, HVAC, and controls, must also be respected.
(2) The benefits of interzonal airflow should be balanced with increasing fan energy consumption. The results of this work indicate that there is an airflow rate beyond which comfort and energy consumption do not improve significantly. Furthermore, high airflow rates could lead to discomfort from drafts. If sufficient detail is known about interior partitions and openings, these elements can be explicitly modelled. Thus, fan-driven interzonal airflow can be used to compliment natural convection only if there remains a benefit to increased interzonal airflow. This analysis can be carried out with either airflow networks or CFD. However, the modeller must be confident that sufficient detail is available with certainty to justify models with higher resolution.

Rigorous sensitivity analyses are particularly justified if the construction of multiple identical houses will take place, such as in a subdivision or if they are prefabricated and mass-produced.

The specific results from this work suggest that for performance modelling of passive solar houses, the above grade portion should be divided into at least two zones: direct gain and non-direct gain. The use of one zone should be limited to cases in which the house truly exists as a single space or CFD simulations have been performed to indicate that interzonal airflow approaches a level that is equivalent to perfect mixing. The use of multiple zones allows the potential for overheating to be better characterized. For HVAC design purposes, this allows heat to added or removed from each zone, independently, as needed. If a conservative model is required, more zones should be modelled, such that the consequences of poorly distributed solar heat gains can be characterized.

In designing a passive solar house, openness between direct gain zones and the other zones is beneficial. The presence of partition walls should be minimized while ensuring sufficient privacy, thermal mass, and the prevention of strong drafts. The use of fans, as part of the forced air system or otherwise, should be considered, and operated during times of significant interzonal temperature differences. The location, number of zones, and algorithms of HVAC controls must accurately reflect the system that will be installed in the house. During times when non-direct gain zones are being heated and the direct gain zone overheats, air circulation is particularly beneficial. This is akin to the occurrence of simultaneous heating in perimeter zones and cooling in core zones that is sometimes encountered in commercial buildings. However, the distribution of energy becomes more challenging in larger buildings (Balcomb 1983).

The use of controlled shades was shown to have two beneficial effects. First, they allow very large south-facing glazing areas to be used, since a significant portion of the unwanted solar gains can be rejected. Thus, views to the outdoors and daylighting can be improved when the shades are open. Second, intelligently controlled shades have the potential to reduce overheating and improve thermal comfort significantly. If these results are to be applied to commercial buildings, the impact on daylight availability should be a major consideration.

An important distinction must be made with regards to thermal and control zones. The energy performance results would indicate that a model with fewer thermal zones is preferable, but this is merely because fewer zones implies better mixing of air. In fact, the optimal design (for both energy performance and thermal comfort) is to have the high mixing rate associated with fewer zones, and the high resolution of control associated with more zones.

The definitions (and calculation procedures) for energy use and overheating are critical to results. The relative costs of heating and cooling should reflect economic and/or environmental costs, depending on the priority of the stakeholders. Traditional measures of overheating were found to mislead results. Thus a new metric was developed, which simultaneously considers spatial and temporal issues – overheating hour-degrees.

The results of this study demonstrate the importance of using whole-year dynamic simulations over rules of thumb. Rules of thumb cannot possibly capture all design variants, such as zoning and interzonal airflow. Furthermore, they cannot characterize the benefit of innovative and non-traditional low-energy strategies. Thus, a building energy model should be implemented from the start of the design process, possibly with escalating levels of model resolution. The results presented in this paper suggest that a moderate level of detail should be applied to the issues of airflow and zoning even at an early design stage. The common simplification of using a single zone to represent a building could lead to an underestimate of energy consumption.

While results can be highly sensitive to building design, climate, and modelling assumptions, further research could provide specific, though generalized, guidelines on thermal and control zones. Also, the thermal comfort in passive solar homes should be studied, as anecdotal evidence suggests that their occupants are more tolerant and adaptive than occupants of typical buildings (Athienitis and Santamouris 2002). The results of the current work indicate that small increases in the tolerable range of temperatures can lead to significantly lower heating and cooling energy use. The use of more advanced control strategies (e.g. predictive control) should be explored for heating, cooling, ventilation (both interzonal and air exchange with outside) and movable shading (e.g. shades). Finally, the strategic use of natural convection complimented by controlled mechanical mixing between the direct gain zone(s) and non-direct gain zone(s) deserves further research.

Nomenclature

A	area of a partition wall (m^2)
A_i	area of a surface i (m^2)
ΔC	change in heat capacity (J/K)
c	specific heat of a substance (J/kgK)
C_p	specific heat capacity of air (J/kgK)
C_z	heat capacity of zone air (J/K)
d_{OH}	depth of overhang (m)
h_c	convective heat transfer coefficient on either side of the partition wall (W/m^{2}K)
h_i	film coefficient for surface i (W/m^{2}K)
h_g	height of glazing (m)
h_{OH}	overhang height above top of glazing (m)
i	index for node, surface, or zone of interest
k	material conductivity (W/mK)
$\dot{m}$	interzonal mass flow rate (kg/s)
$\dot{m}_i$	mass flow rate from zone i (kg/s)
$\dot{m}_{inf}$	mass flow rate from infiltration (kg/s)
$\dot{m}_{sys}$	supply mass flow rate (kg/s)
N_{sl}	number of convective sources of internal gains
$N_{surfaces}$	number of surfaces in the zone
N_{zones}	number of zones in the model
R	thermal resistance of the partition wall between zones (m^{2}K/W)
RH_{amb}	outdoor relative humidity
ΔT	temperature change (K)
t	time (s)
T_{amb}	ambient temperature (°C)
$T_{i,new}$	node i temperature at the current timestep (°C)
$T_{i,old}$	node i temperature at the previous timestep (°C)
$T_{i-1,new}$	node $i-1$ temperature at the current timestep (°C)
$T_{i+1,new}$	node $i+1$ temperature at the current timestep (°C)
T_{si}	surface i temperature (°C)
T_{supply}	system supply air temperature (°C)
T_{zi}	zone i air temperature (°C)
T_z	current zone air node temperature (°C)
T_z^t	current zone air node temperature at time t (°C)
T_∞	outdoor air temperature (°C)
$U_{12,air}$	rate of heat transfer between adjacent zones through air exchange (W/K)
$U_{12,wall}$	rate of heat transfer between air nodes in adjacent zones (W/K)
V	volume of substance (m^3)
Δx	control volume thickness (i.e. node-to-node distance) (m)

Greek symbols

α_{min}	minimum annual solar altitude (Winter solstice) (deg)
α_{max}	maximum annual solar altitude (Summer solstice) (deg)
δt	timestep duration (s)
ρ	material mass density (kg/m^3)

Acknowledgements

This work was funded by the Solar Buildings Research Network – a strategic NSERC (Natural Sciences and Engineering Research Council of Canada) research network. Additional support through a grant-in-aid for W. O'Brien from the American Society of Heating, Refrigeration, and Air-Conditioning Engineers is also acknowledged. Special thanks to Nina Doré for thoroughly editing this work.

References

American Society of Heating Refrigeration and Air Conditioning Engineers (ASHRAE), 2005. *2005 ASHRAE handbook of fundamentals: SI Edition*. Atlanta, GA: ASHRAE.

Armstrong, M.M., *et al.*, 2009. Synthetically derived profiles for representing occupant-driven electric loads in Canadian housing. *Journal of Building Performance Simulation*, 2 (1), 15–30.

Athienitis, A. and Santamouris, M., 2002. *Thermal analysis and design of passive solar buildings*. London: James & James.

Athienitis, A.K., 2007. Design of a solar home with BIPV-thermal system and ground source heat pump. *2nd SBRN and SESCI 32nd Joint Conference*, Calgary, AB.

Balcomb, J.D., 1983. Heat storage and distribution inside passive-solar buildings. *International conference on passive and low energy architecture*, Crete, Greece, 27 June 1983.

Balcomb, J.D., *et al.*, 1977. Simulation analysis of passive solar heated buildings – preliminary results. *Solar Energy*, 19 (3), 277–282.

Besant, R.W., *et al.*, 1979. The Saskatchewan conservation house: some preliminary performance results. *Energy and Buildings*, 2 (2), 163–174.

Canada Mortgage and Housing Corporation (CMHC), 1998. *Tap the sun passive solar techniques and home designs*, CHMC.

CANMET Energy Technology Centre (CETC), 2008. *HOT3000*, Natural Resources Canada.

Chen, Y.X., *et al.*, 2010. Modeling, design and thermal performance of a BIPV/T system thermally coupled with a ventilated concrete slab in a low energy solar house: Part 1, BIPV/T system and house energy concept. *Solar Energy*, 84 (11), 1892–1907.

Chen, Y.X, *et al.*, 2010. Modeling, design and thermal performance of a BIPV/T system thermally coupled with a ventilated concrete slab in a low energy solar house: Part 2, ventilated concrete slab. *Solar Energy*, 84 (11), 1908–1919.

Clarke, J., 2001. *Energy simulation in building design*. Oxford: Butterworth-Heinemann.

Deru, M. and Torcellini, P., 2007. Source energy and emission factors for energy use in buildings. *Battelle: national renewable energy laboratory*, US Department of Energy.

EnergyPlus, 2009. *EnergyPlus Engineering Reference*.

Feustel, H.E. and Dieris, J. 1992. A survey of airflow models for multizone structures. *Energy and Buildings*, 18 (2), 79–100.

Galloway, T., 2004. *Solar house: a guide for the solar designer*. Oxford, UK: Architectural Press.

Gusdorf, J., *et al*., 2010. The Impact of ECM furnace motors on natural gas use and overall energy use during the heating season at CCHT research facility. National Research Council, Canada, 1–18.

Hayter, S.J., *et al*., 2001. The energy design process for designing and constructing high-performance buildings. *CLIMA 2000*, Naples, Italy.

Hensen, J.L.M., *et al*., 1991. On the thermal interaction of building structure and heating and ventilating system. *Technische Universiteit Eindhoven*.

Hestnes, A., *et al*., 2003. *Solar energy houses: strategies, technologies, examples*. London: Earthscan/James & James.

Huizenga, C., *et al*., 2005. WINDOW5. Berkeley, CA: Lawrence Berkeley National Laboratories.

National Renewable Energy Laboratory (NREL), 2009. *BEopt*. Golden, Colorado.

Natural Resources Canada (NRCan), 2010. *Thermostats for Heat Pumps*. Available from http://oee.nrcan.gc.ca/residential/personal/thermostats-controls.cfm?attr=4#zoneControl [Accessed 18 July 2010].

Newsham, G.R., 1994. Manual control of window blinds and electric lighting: implications for comfort and energy consumption. *Indoor and Built Environment*, 3 (3), 135.

Reed, W.G. and Gordon, E.B., 2000. Integrated design and building process: what research and methodologies are needed? *Building Research and Information*, 28 (5–6), 325–337.

Robinson, D. and Haldi, F., 2008. Model to predict overheating risk based on an electrical capacitor analogy. *Energy & Buildings*, 40 (7), 1240–1245.

Sahlin, P., 2003. On the effects of decoupling airflow and heat balance in building simulation models. *ASHRAE Transactions*, 109 (2), 788–800.

Sherman, M.H., 1987. Estimation of infiltration from leakage and climate indicators. *Energy and Buildings*, 10 (1), 81–86.

Simonson, C., 2005. Energy consumption and ventilation performance of a naturally ventilated ecological house in a cold climate. *Energy and Buildings*, 37 (1), 23–35.

Taylor, R., Pedersen, C., and Lawrie, L., 1990. Simultaneous simulation of buildings and mechanical systems in heat balance based energy analysis programs. *Third international conference on system simulation in buildings*. 1990, Liege, Belgium.

U.S Department of Energy (US DOE), 2009. *Getting started with EnergyPlus*, Department of Energy.

Warren, P., 1996. Summary of IEA Annex 23 – multizone airflow modelling (COMIS).